EuroIntervention 2012;7:1310-1316

Optimal diameter of diseased bifurcation segment: a practical rule for percutaneous coronary intervention

Yunlong Huo[1], PhD; Gérard Finet[2], MD; Thierry Lefèvre[3], MD; Yves Louvard[3], MD; Issam Moussa[4], MD; Ghassan S. Kassab[1,5,6]*, PhD

1. Department of Biomedical Engineering, Indiana University Purdue University Indianapolis, Indianapolis, IN, USA; 2. Department of Interventional Cardiology, Cardiovascular Hospital and Claude Bernard University, Lyon, France; 3. Institut Cardiovasculaire Paris Sud, Massy, France; 4. Department of Cardiology, Cornell University, Ithaca, NY, USA; 5. Surgery, IUPUI, Indianapolis, IN, USA; 6. Cellular and Integrative Physiology, IUPUI, Indianapolis, IN, USA

KEYWORDS

- bifurcation diameter relationship
- PCI
- diameter ratio

Abstract

Aims: The percutaneous repair of a diseased segment should consider the dimensions of other segments of a bifurcation in order to ensure the optimality of flow through the bifurcation. The question is, if the diameters of two segments of a bifurcation are known, can an optimal diameter of the third diseased segment be determined such that the bifurcation has an optimal geometry for flow transport? Various models (i.e., Murray, Finet, area-preservation and HK models) that express a diameter relationship of the three segments of a bifurcation have been proposed to answer the question.

Methods and results: In this study the four models were compared with experimental measurements on epicardial coronary bifurcations of patients and swine. The HK model is found to be in agreement with morphometric measurements of all bifurcation types and is based on the minimum energy hypothesis while Murray and area-preservation models are in agreement with experimental measurements for bifurcations with daughter diameter ratio (i.e., $\frac{\text{small daughter diameter}}{\text{large daughter diameter}}$) ≤ 0.25 and Finet model is in agreement for bifurcations with daughter diameter ratio ≥ 0.75.

Conclusions: The HK model provides a comprehensive rule for the percutaneous reconstruction of the diameters of diseased vessels and has a physical basis.

**Corresponding author: Department of Biomedical Engineering, Indiana University Purdue University Indianapolis, Indianapolis, IN 46202, USA. E-mail: gkassab@iupui.edu*

DOI: 10.4244/EIJV7I11A206

Introduction

Percutaneous coronary intervention (PCI) attempts to restore the lumen area of a diseased artery to "normal" reference dimension through percutaneous transluminal coronary angioplasty (PTCA) or stenting. As atherosclerosis often stems from the junction of a bifurcation[1] and diffuses over the vessel length[8,12,13], the question becomes what is the therapeutic target diameter of the diseased vessel to restore flow optimality to a bifurcation. In other words, if the diameters of two segments of a "normal" bifurcation are known, can an optimal diameter of the third segment be determined to ensure an optimal flow through the bifurcation?

It has long been established that there is an optimal relationship between the diameters of the three segments of a bifurcation. **Table 1** lists the most commonly referenced bifurcation models that provide a mathematical relationship between the three segments of a bifurcation (i.e., D_m, D_l and D_s for the diameters of mother, large and small daughters, respectively). In 1926, Murray was the first to derive a cubed relationship between the mother and two daughter vessels[11]. The premise of Murray's derivation is the minimum energy hypothesis; i.e., the power for transport of blood through a bifurcation is minimised. This is the principle of efficiency where departure from which requires greater energy dissipation. Huo and Kassab[7] recently showed a similar relationship based on the same premise in a tree structure, but found an exponent of $\frac{7}{3}$ instead of 3 in the Murray model. Finet et al[3] proposed an empirical fractal-like rule. An additional expression stemming from area conservation (exponent of 2) has traditionally been invoked for the vasculature[9].

The objective of this study is to validate the four models **(Table 1)** based on the angiographic and cast data of the epicardial coronary bifurcations in humans and swine, respectively. The most accurate rule based on a physical and physiological principle can then be used to determine the desired diameter of a diseased segment when the diameters of the two other segments in a bifurcation are known for percutaneous treatment of lesions.

Methods

THEORETICAL MODELS

The Murray, Finet, area-preservation (AP), and HK bifurcation diameter models are shown in **Table 1**. The stepwise difference between mother and large daughter vessels (i.e., $D_m - D_l$) is a fundamental parameter for the prediction of incomplete apposition of stent strut[3], which was observed in more than 60% of non-left main bifurcation lesions[2]. Therefore, we determine the mother-daughter ratio $\frac{D_m}{D_l+D_s}$ as a function of the daughter diameter ratio $\frac{D_s}{D_l}$ (see detailed derivation in the Appendix) for the four theoretical models in **Table 1**, which can be angiographically used to identify the optimal stepwise difference in an epicardial coronary bifurcation. **Figure 1** shows coronary bifurcations with large and small daughter diameter ratios. A comparison of the four theoretical models was carried out for the epicardial coronary bifurcations, as the daughter diameter ratio increases from zero to unity.

Table 1. Bifurcation diameter models and the corresponding physical mechanisms.

Bifurcation diameter models	Relationship	Physical mechanisms
HK	$D_m^{\frac{7}{3}} = D_l^{\frac{7}{3}} + D_s^{\frac{7}{3}}$	Minimum Energy
Finet	$D_m = 0.678 \times (D_l + D_s)$	"Fractal"-type relation
Murray	$D_m^3 = D_l^3 + D_s^3$	Minimum Energy & WSS ~ Constant
Area-preservation	$D_m^2 = D_l^2 + D_s^2$	Velocity ~ Constant

where D_m, D_l, and D_s are the diameters of mother, larger and smaller daughter vessels, respectively.

MORPHOMETRIC DATA AND STATISTICAL ANALYSIS

The epicardial coronary bifurcations of human and swine, quantitatively determined by angiography and intravascular ultrasound[3] and casts[10], respectively; were used to assess the four bifurcation diameter models in **Table 1**. Variables were presented as mean ± standard error (SE). We also determined the relative error (i.e., $\%Error_{HK} = \frac{\left(D_l^{\frac{7}{3}} + D_s^{\frac{7}{3}}\right)^{\frac{3}{7}} - D_m}{D_m} \times 100\%$ for HK model; $\%Error_{Finet} = \frac{(D_l + D_s) \cdot 0.678 - D_m}{D_m} \times 100\%$

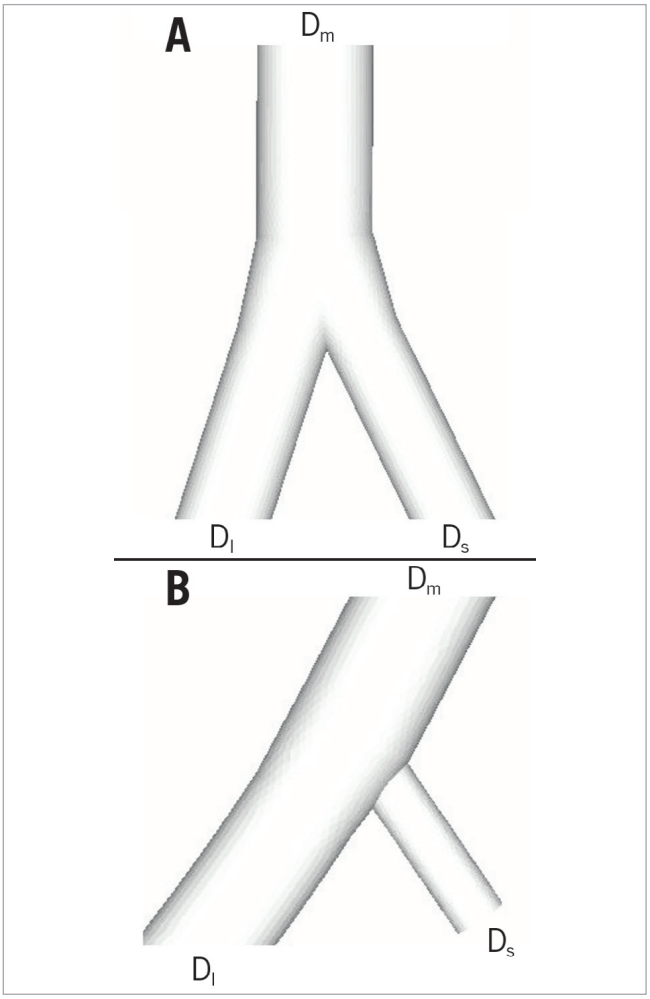

Figure 1. *Schematic representation of bifurcations with (A) large and (B) small daughter diameter ratios.*

for Finet model; $\%Error_{Murray}=\frac{\sqrt[3]{D_l^3+D_s^3}-D_m}{D_m}\times100\%$ for Murray model; and $\%Error_{AP}=\frac{\sqrt{D_l^2+D_s^2}-D_m}{D_m}\times100\%$ for AP model) between the predictions of the four models in **Table 1** and the measurements. A two-way ANOVA was performed on the population of samples between theoretical models and experimental measurements, where $p<0.05$ represented statistically significant differences.

Results

Figure 2 shows the mother-daughter diameter ratio as a function of the daughter diameter ratio obtained from the four bifurcation diameter models in **Table 1** (i.e., Equations 1-4). Accordingly, **Table 2** shows the mother-daughter diameter ratio determined by the HK, Murray, and AP models (i.e., Equations 1-3, respectively), which has the corresponding mean ± SE values of 0.676±0.001, 0.634±0.002, and 0.710±0.001 for bifurcations with the daughter diameter ratio ≥0.75 and 0.9±0.028, 0.895±0.03, and 0.903±0.027 for bifurcations with the daughter diameter ratio ≤0.25. This is in comparison with the Finet model that predicts a constant value of 0.678.

For patients, **Table 3** shows the relative errors (i.e., $\%Error_{HK}$, $\%Error_{Finet}$, $\%Error_{Murray}$, and $\%Error_{AP}$) between the predictions of the four models in **Table 1** and the measurements by quantitative human coronary bifurcation angiography (see Table 1 in Finet et al[3]). Moreover, **Table 4** shows the relative errors between the predictions of the four models in **Table 1** and the morphometric measurements in the swine epicardial LAD tree with mother diameters ≥0.5 mm obtained from the casts of Kassab et al[10]. **Figure 3** also shows the relative error as a function of the daughter diameter ratio corresponding to **Table 4**.

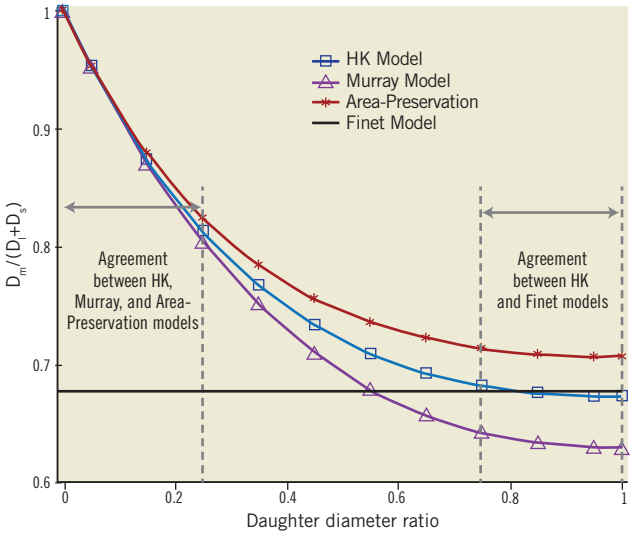

Figure 2. *The relationship between the mother-daughter diameter ratio and daughter diameter ratio determined by Equations 1-4.*

Discussion

Atherosclerotic lesions tend to predominate around epicardial coronary bifurcations[1,6,7]. A bifurcation diameter relationship of "normal" reference is needed to restore the diameter of diseased vessel for optimal flow through the epicardial coronary bifurcation[3,4]. Here, we evaluated four bifurcation diameter models (summarised in **Table 1**) using the morphometric data from patients and swine. The major finding is that the HK and Finet models agree well with the measurements for coronary bifurcations of larger daughter diameter ratios while the HK, Murray and AP models are consistent with the experimental results for coronary bifurcations of smaller daughter diameter ratios. Hence, we conclude that the HK model is the only rule that accurately describes bifurcations of all daughter diameter ratios in the normal swine and human epicardial coronary arterial tree.

Finet et al[3] have empirically shown that the mother-daughter diameter ratio $\frac{D_m}{D_l+D_s}$ is 0.678 in the large epicardial coronary arterial tree, based on quantitative coronary angiography and intravascular ultrasound measurements. The Finet model agrees with the experimental measurements much better than the Murray and AP models[3]. Moreover,

Table 2. Mother-daughter diameter ratio $\frac{D_m}{D_l+D_s}$ determined by the HK, Murray, and AP models (i.e., Equations [1-3], respectively) for bifurcations with daughter diameter ratio $\frac{D_s}{D_l}\geq0.75$ and $\frac{D_s}{D_l}\leq0.25$.

$\frac{D_s}{D_l}$	$\frac{D_m}{D_l+D_s}$			$\frac{D_s}{D_l}$	$\frac{D_m}{D_l+D_s}$		
	HK	Murray	AP		HK	Murray	AP
0.75	0.682	0.643	0.714	0.25	0.813	0.804	0.825
0.8	0.678	0.638	0.711	0.2	0.842	0.836	0.850
0.85	0.676	0.634	0.709	0.15	0.874	0.871	0.879
0.9	0.674	0.632	0.708	0.1	0.911	0.909	0.914
0.95	0.673	0.630	0.707	0.05	0.953	0.952	0.954
1	0.673	0.630	0.707	0	1	1	1
Mean±SE	0.676±0.001	0.634±0.002	0.710±0.001	Mean±SE	0.9±0.028	0.895±0.03	0.903±0.027
Only the HK model (Eq. 1) shows good agreement with the Finet model (Eq. 4) in bifurcations with $\frac{D_s}{D_l}\geq0.75$ (i.e., 0.676 vs. 0.678).							

Table 3. Relative errors between predictions of bifurcation diameter models and measurements of quantitative human coronary bifurcation angiography in Table 1 of Finet et al [3], 2008.

Mother vessel	%Error$_{HK}$	%Error$_{Finet}$	%Error$_{Murray}$	%Error$_{AP}$	n
$4.5 \le D_m$	–0.57	–0.36	–6.68	4.34	21
$4 \le D_m < 4.5$	–0.87	–0.58	–7.0	4.04	24
$3.5 \le D_m < 4$	0.44	0.48	–5.65	5.35	18
$3 \le D_m < 3.5$	–2.45	–2.59	–8.29	2.72	43
$2.5 \le D_m < 3$	3.57	3.65	–2.73	8.65	33
$D_m \le 2.5$	3.67	4.08	–2.79	8.83	35
For all	0.25	0.39	–5.88	5.18	173

$\%Error_{HK}=\frac{\left(D_l^{\frac{7}{3}}+D_s^{\frac{7}{3}}\right)^{\frac{3}{7}}-D_m}{D_m}\times 100\%$ for HK model;

$\%Error_{Finet}=\frac{(D_l+D_s)\cdot 0.678-D_m}{D_m}\times 100\%$ for Finet model;

$\%Error_{Murray}=\frac{\sqrt[3]{D_l^3+D_s^3}-D_m}{D_m}\times 100\%$ for Murray model;

and $\%Error_{AP}=\frac{\sqrt{D_l^2+D_s^2}-D_m}{D_m}\times 100\%$ for area-preservation model. "n" represents number of measurements.

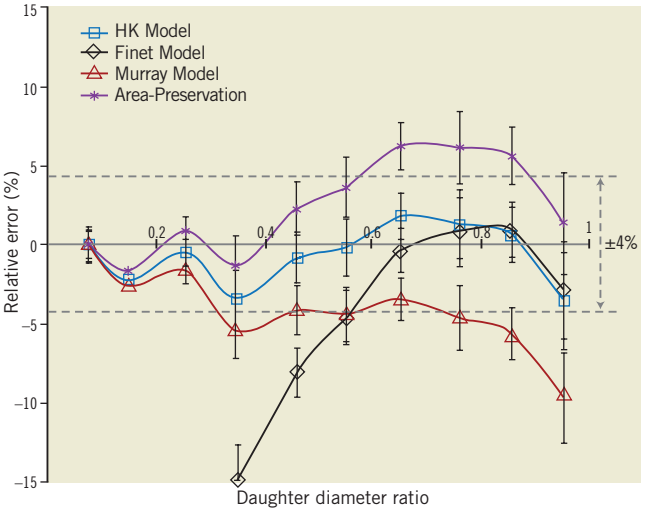

Figure 3. *The relative error as a function of the daughter diameter ratio by fitting of experimental measurements to the HK, Finet, Murray and AP bifurcation diameter models corresponding to Table 4. Only the prediction of the HK model is within ±4% error of actual value throughout the range of bifurcations.*

based on the minimum energy hypothesis, Huo and Kassab[7] theoretically modified the Murray model as $D_m^{\frac{7}{3}}=D_l^{\frac{7}{3}}+D_s^{\frac{7}{3}}$, which was validated in various vascular trees down to the pre-capillary arterioles in different organs and species. As shown in **Table 3**, the HK model also agreed well with the experimental measurements of Finet model. This suggests that there should be a relationship between the Finet and HK models, which is verified in the present study.

Equations 1-4 in the Appendix show the mathematical relationships between the four bifurcation diameter models in **Table 1**. The daughter diameter ratio $\frac{D_s}{D_l}\rightarrow 1$ or $\frac{D_s}{D_l}\rightarrow 0$ leads to different mother-daughter diameter ratios, as shown in **Figure 2** and **Table 2**. From the HK model, the mother-daughter diameter ratio in bifurcations with $\frac{D_s}{D_l}\ge 0.75$ equals to 0.676, which is very similar to 0.678 of the Finet model. From the study of Finet et al[3], the daughter diameter

Table 4. Relative errors between predictions of bifurcation diameter models and measurements in the swine LAD tree with mother diameters ≥0.5 mm obtained from the cast data of Kassab et al[10], 1993.

D_s/D_l	% Error$_{HK}$	% Error$_{Finet}$	% Error$_{Murray}$	% Error$_{AP}$	n
$D_s/D_l \le 0.1$	–0.11±0.99*	–27.31±0.78*+¶	–0.21±0.99+	0.07±1.00¶	53
$0.1 < D_s/D_l \le 0.2$	–2.25±0.60*	–24.45±0.48*+¶	–2.63±0.60+	–1.67±0.15¶	92
$0.2 < D_s/D_l \le 0.3$	–0.54±0.81*	–16.92±0.68*+¶	–1.71±0.80+	0.87±0.82¶	76
$0.3 < D_s/D_l \le 0.4$	–3.48±1.79*	–14.93±1.63*¶	–5.50±1.75‡	–1.33±1.84¶‡	42
$0.4 < D_s/D_l \le 0.5$	–0.88±1.63	–8.12±1.54¶	–4.17±1.57‡	2.24±1.69¶‡	33
$0.5 < D_s/D_l \le 0.6$	–0.21±1.80	–4.65±1.72	–4.46±1.73‡	3.58±1.87‡	21
$0.6 < D_s/D_l \le 0.7$	1.74±1.44#	–0.42±1.41¶	–3.49±1.36#‡	6.16±1.50¶‡	35
$0.7 < D_s/D_l \le 0.8$	1.24±2.18#	0.74±2.17¶	–4.66±2.05#‡	6.05±2.28¶‡	17
$0.8 < D_s/D_l \le 0.9$	0.57±1.75#	0.92±1.67+	–5.65±1.64#+‡	5.56±1.83‡	15
$0.9 < D_s/D_l$	–3.62±3.06#$	–2.94±3.09+	–9.75±2.87#+‡	1.26±1.30$‡	17
Mean ±SE	–0.75±0.58	–9.81±3.31	–4.22±0.82	2.28±0.93	401
Mean ±SE for absolute values	1.46±0.41	10.14±3.20	4.22±0.82	2.88±0.73	401

$\%Error_{HK}=\frac{\left(D_l^{\frac{7}{3}}+D_s^{\frac{7}{3}}\right)^{\frac{3}{7}}-D_m}{D_m}\times 100\%$ for HK model; $\%Error_{Finet}=\frac{(D_l+D_s)\cdot 0.678-D_m}{D_m}\times 100\%$ for Finet model; $\%Error_{Murray}=\frac{\sqrt[3]{D_l^3+D_s^3}-D_m}{D_m}\times 100\%$ for Murray model;

and $\%Error_{AP}=\frac{\sqrt{D_l^2+D_s^2}-D_m}{D_m}\times 100\%$ for area-preservation model.Symbols *, #, $, +, ¶, ‡ represent the significant difference ($p<0.05$) determined by two-way ANOVA for the relative errors of HK vs. Finet, HK vs. Murray, HK vs. AP, Finet vs. Murray, Finet vs. AP, and Murray vs. AP, respectively. "n" represents number of measurements.

Table 5. Diameter relationship and stepwise difference (i.e.,) determined by the HK model.

Diameter of smaller daughter vessel	Diameter of larger daughter vessel (in terms of the main stent sizes in use)							
(mm)	2.25	2.50	2.75	3.00	3.25	3.50	3.75	4.00
2.25	**3.03**	**3.20**	**3.39**	**3.58**	**3.78**	**3.99**	**4.20**	**4.42**
	Δ=0.78	Δ=0.70	Δ=0.64	Δ=0.58	Δ=0.53	Δ=0.49	Δ=0.45	Δ=0.42
2.50		**3.36**	**3.54**	**3.72**	**3.91**	**4.11**	**4.32**	**4.53**
		Δ=0.86	Δ=0.79	Δ=0.72	Δ=0.66	Δ=0.61	Δ=0.57	Δ=0.53
2.75			**3.70**	**3.87**	**4.06**	**4.25**	**4.44**	**4.64**
			Δ=0.95	Δ=0.87	Δ=0.81	Δ=0.75	Δ=0.69	Δ=0.64
3.00				**4.04**	**4.21**	**4.39**	**4.58**	**4.77**
				Δ=1.04	Δ=0.96	Δ=0.89	Δ=0.83	Δ=0.77
3.25					**4.37**	**4.55**	**4.73**	**4.91**
					Δ=1.12	Δ=1.05	Δ=0.98	Δ=0.91
3.50						**4.71**	**4.88**	**5.06**
						Δ=1.21	Δ=1.13	Δ=1.06
3.75							**5.05**	**5.22**
							Δ=1.30	Δ=1.22
4.00								**5.38**
								Δ=1.38

The red and blue colours represent the diameter of mother segment and stepwise difference, respectively.

ratio was 0.828±0.024 (mean ±SD) so that the HK model is consistent with the empirical Finet model, as shown in **Table 3**. **Figure 2** shows that the mother-daughter diameter ratio determined by Equation 1, however, deviates from the prediction of Finet model as the daughter diameter ratio decreases away from 0.75. In particular, the mother-daughter diameter ratio determined by the HK, Murray, and AP models become very similar when $\frac{D_s}{D_l} \leq 0.25$. Accordingly, **Table 2** shows the mother-daughter diameter ratio increases from about 0.8 to unity as the daughter diameter ratio $\frac{D_s}{D_l}$ decreases monotonically from 0.25 to zero, which is significantly larger than the prediction of the Finet model. Hence, the Finet model is in gross error for coronary bifurcations with $\frac{D_s}{D_l} < 0.75$, which were not considered in their study as they are less relevant clinically.

Examples:

1) Input values for D_m and D_l:

D_m: 5 D_l: 4 D_s: Calculate

After clicking button "Calculate", D_s will be determined as follows:

D_m: 5 D_l: 4 D_s: 3.397

2) Input values for D_m and D_s:

D_m: 4 D_l: D_s: 2 Calculate

After clicking button "Calculate", D_l will be determined as follows:

D_m: 4 D_l: 3.638 D_s: 2

3) Input values for D_l and D_s:

D_m: D_l: 3.5 D_s: 2.5 Calculate

After clicking button "Calculate", D_m will be determined as follows:

D_m: 4.112 D_l: 3.5 D_s: 2.5

Figure 4. *The diameter relationship determined by the HK model.*

To accurately and critically evaluate the four models in **Table 1**, we used morphometric data from the casts of swine epicardial coronary arterial bifurcations[10]. As shown in **Figure 3** and **Table 4**, the HK model agrees well with the measurements for all daughter diameter ratios (±4% error); the Murray and AP models agree with the measurements when $\frac{D_s}{D_l} \leq 0.25$; and the Finet model agrees with the measurements when $\frac{D_s}{D_l} \geq 0.65$, but not for other daughter diameter ratios. The comparison between theoretical models and morphometric measurements supports the HK model that is derived based on a physical principle.

PRACTICAL APPLICATION

A practical question is how can the validated HK model be translated into clinical practice to restore diseased bifurcations to optimal dimensions? A website (http://www.et.iupui.edu/cnc/refdiacalculation.aspx) has been set up, which allows the determination of a diameter of any of the three segments of a bifurcation if two of the diameters are entered, as outlined in **Figure 4**. There is an entry blank for each segment. Once two of the entries are input, one can click the button "Calculate" to yield the third segment according to the HK model. This website can be downloaded to an iPhone, Blackberry, etc., providing a quick and easy rule to determine the reference diameter of a bifurcation for sizing of balloons or stents.

An additional approach is to provide a simple look-up chart as demonstrated in **Table 5**. The table contains the relationship between the mother and daughter bifurcation diameters as well as the stepwise of diameters between mother and large daughter vessels. The double-entry system in the table can be easily used to determine the diameter of mother vessel (red colour) and the stepwise difference (blue colour) based on the measured two daughter vessels.

Conclusions

This study confirmed the following conclusions:

1) The HK model accurately predicts all bifurcation types (e.g., epicardial coronary bifurcations of all daughter diameter ratios) and is based on minimum energy hypothesis;
2) The Murray and AP models are in agreement with the morphometric measurements only for bifurcations of smaller daughter diameter ratios ($\frac{D_s}{D_l} \leq 0.25$);
3) The Finet model is in agreement only for bifurcations of larger daughter diameter ratios ($\frac{D_s}{D_l} \geq 0.75$);
4) We have designed an easy-to-use website to determine the 3rd diameter of a bifurcation (based on the HK model) that can be downloaded to an iPhone, Blackberry, etc. as well as a look-up table.

Acknowledgement

This research is supported in part by the National Institute of Health-National Heart, Lung, and Blood Institute Grants R01-HL092048 (GS Kassab) and the AHA Scientist Development Grant 0830181N (Y Huo).

Appendix

Based on the four models in **Table 1**, the mother-daughter diameter ratio is expressed as a function of the daughter diameter ratio, where D_m, D_l and D_s are the diameters of mother, large and small daughters, respectively.

1) From the HK mode, the relationship between $\frac{D_m}{D_l+D_s}$ and $\frac{D_s}{D_l}$ is given as:

$$\begin{cases} \frac{D_m}{D_l+D_s} = \left(\frac{D_m^{\frac{7}{3}}}{(D_l+D_s)^{\frac{7}{3}}}\right)^{\frac{3}{7}} \Rightarrow \frac{D_m}{D_l+D_s} = \left(\frac{D_l^{\frac{7}{3}}+D_s^{\frac{7}{3}}}{(D_l+D_s)^{\frac{7}{3}}}\right)^{\frac{3}{7}} = \left(\frac{1+\left(\frac{D_s}{D_l}\right)^{\frac{7}{3}}}{\left(1+\frac{D_s}{D_l}\right)^{\frac{7}{3}}}\right)^{\frac{3}{7}} \\ D_m^{\frac{7}{3}} = D_l^{\frac{7}{3}} + D_s^{\frac{7}{3}} \end{cases} \quad [1]$$

2) From the Murray mode, the relationship between $\frac{D_m}{D_l+D_s}$ and $\frac{D_s}{D_l}$ is given as:

$$\begin{cases} \frac{D_m}{D_l+D_s} = \sqrt[3]{\frac{D_m^3}{(D_l+D_s)^3}} \Rightarrow \frac{D_m}{D_l+D_s} = \sqrt[3]{\frac{D_l^3+D_s^3}{(D_l+D_s)^3}} = \sqrt[3]{\frac{1+\left(\frac{D_s}{D_l}\right)^3}{\left(1+\frac{D_s}{D_l}\right)^3}} \\ D_m^3 = D_l^3 + D_s^3 \end{cases} \quad [2]$$

3) From the AP mode, the relationship between $\frac{D_m}{D_l+D_s}$ and $\frac{D_s}{D_l}$ is given as:

$$\begin{cases} \frac{D_m}{D_l+D_s} = \sqrt{\frac{D_m^2}{(D_l+D_s)^2}} \Rightarrow \frac{D_m}{D_l+D_s} = \sqrt{\frac{D_l^2+D_s^2}{(D_l+D_s)^2}} = \sqrt{\frac{1+\left(\frac{D_s}{D_l}\right)^2}{\left(1+\frac{D_s}{D_l}\right)^2}} \\ D_m^2 = D_l^2 + D_s^2 \end{cases} \quad [3]$$

4) Finet model is given as:

$$\frac{D_m}{D_l+D_s} = 0.678 \quad [4]$$

Equations 1-3 represent the ratio $\frac{D_m}{D_l+D_s}$ as a function of the daughter diameter ratio $\frac{D_s}{D_l}$ derived from the HK, Murray, and AP models, respectively. As the daughter diameter ratio approaches one, Equations 1-3 give 0.673, 0.63, and 0.707 for the HK, Murray, and AP models, respectively. Alternatively, as the daughter diameter ratio approaches zero, Equations 1-3 give one for the HK, Murray, and AP models, respectively.

Conflict of interest statement

The authors have no conflict of interest to declare.

References

1. Asakura T, Karino T. Flow patterns and spatial distribution of atherosclerotic lesions in human coronary arteries. *Circ Res*. 1990;66:1045-66.

2. Costa RA, Mintz GS, Carlier SG, Lansky AJ, Moussa I, Fujii K, Takebayashi H, Yasuda T, Costa JR Jr, Tsuchiya Y, Jensen LO, Cristea E, Mehran R, Dangas GD, Iyer S, Collins M, Kreps EM, Colombo A, Stone GW, Leon MB, Moses JW. Bifurcation coronary lesions treated with the "crush" technique: an intravascular ultrasound analysis. *J Am Coll Cardiol*. 2005; 46:599-605.

3. Finet G, Gilard M, Perrenot B, Rioufol G, Motreff P, Gavit L, Prost R. Fractal geometry of arterial coronary bifurcations: a quan-

titative coronary angiography and intravascular ultrasound analysis. *EuroIntervention*. 2008;3:490-8.

4. Finet G, Huo Y, Rioufol G, Ohayon J, Guerin P, Kassab GS. Structure-function relation in the coronary artery tree: from fluid dynamics to arterial bifurcations. *EuroIntervention*. 2010;6:J10-5.

5. Huo Y, Wischgoll T, Kassab GS. Flow patterns in three-dimensional porcine epicardial coronary arterial tree. *Am J Physiol Heart Circ Physiol*. 2007;293:H2959-70.

6. Huo Y, Choy JS, Svendsen M, Sinha AK, Kassab GS. Effects of vessel compliance on flow pattern in porcine epicardial right coronary arterial tree. *J Biomech*. 2009;42:594-602.

7. Huo Y, Kassab GS. A scaling law of vascular volume. *Biophys J*. 2009;96:347-53.

8. Issam M & Colombo A. Tips and Tricks in Interventional Therapy of Coronary Bifurcation Lesions. (Informa Healthcare: 2010).

9. Kamiya A, Togawa T. Optimal branching structure of the vascular tree. *Bull Math Biophys*. 1972;34:431-8.

10. Kassab GS, Rider CA, Tang NJ, Fung YC. Morphometry of pig coronary arterial trees. *Am J Physiol*. 1993;265:H350-65.

11. Murray CD. The Physiological principle of minimum work: I. The vascular system and the cost of blood volume. *Proc Natl Acad Sci U S A*. 1926;12:207-14.

12. Stary HC, Chandler AB, Glagov S, Guyton JR, Insull W Jr, Rosenfeld ME, Schaffer SA, Schwartz CJ, Wagner WD, Wissler RW. A definition of initial, fatty streak, and intermediate lesions of atherosclerosis. A report from the Committee on Vascular Lesions of the Council on Arteriosclerosis, American Heart Association. *Circulation*. 1994;89:2462-78.

13. Stary HC, Chandler AB, Dinsmore RE, Fuster V, Glagov S, Insull W Jr, Rosenfeld ME, Schwartz CJ, Wagner WD, Wissler RW. A definition of advanced types of atherosclerotic lesions and a histological classification of atherosclerosis. A report from the Committee on Vascular Lesions of the Council on Arteriosclerosis, American Heart Association. *Circulation*. 1995;92:1355-74.